

Echelle spectroscopy of Ca II HK activity in Southern Hemisphere planet search targets

C. G. Tinney,¹* Chris McCarthy,² Hugh R. A. Jones,³ R. Paul Butler,² Brad D. Carter,⁴ Geoffrey W. Marcy^{5,6} and Alan J. Penny⁷

¹Anglo-Australian Observatory, PO Box 296, Epping, NSW 1710, Australia

²Carnegie Institution of Washington, Department of Terrestrial Magnetism, 5241 Broad Branch Rd NW, Washington, DC 20015-1305, USA

³Astrophysics Research Institute, Liverpool John Moores University, Twelve Quays House, Egerton Wharf, Birkenhead CH41 1LD

⁴Faculty of Sciences, University of Southern Queensland, Toowoomba, Qld 4350, Australia

⁵Department of Astronomy, University of California, Berkeley, CA 94720, USA

⁶Department of Physics and Astronomy, San Francisco State University, San Francisco, CA 94132, USA

⁷Rutherford Appleton Laboratory, Chilton, Didcot, Oxon OX11 0QX

Accepted 2002 January 18. Received 2002 January 9; in original form 2001 October 31

ABSTRACT

We present the results of ultraviolet echelle spectroscopy of a sample of 59 F, G, K and M stars from the Anglo-Australian Planet Search target list. Ca II activity indices, which are essential in the interpretation of planet detection claims, have been determined for these stars and placed on the Mount Wilson R'_{HK} system.

Key words: stars: activity – stars: low-mass, brown dwarfs – planetary systems – ultraviolet: stars.

1 INTRODUCTION

Extensive planet search programmes are now operating on a variety of telescopes around the world, including the 3.9-m Anglo-Australian Telescope (Tinney et al. 2001; Butler et al. 2001), the 10-m Keck I (Vogt et al. 2000), the Lick 3-m (Fischer et al. 2001), the Leonard Euler 1.2-m (Naef 2001) and ESO Coudé Auxiliary Telescopes (Kürster et al. 2000) at La Silla, and the Observatoire de Haute-Provence 1.9-m (Queloz et al. 1998). These programmes reach velocity precisions ranging from 15 to 3 m s^{-1} . At these levels apparent velocity variability (known as jitter), which is intrinsic to the target star itself (rather than the presence of an unseen companion), can be produced by the effects of stellar activity and rapid rotation combined with surface inhomogeneity (Saar, Butler & Marcy 1998; Saar & Fischer 2000; Santos et al. 2000).

The level of stellar activity in solar-type stars is commonly examined by measuring the strength of chromospheric emission features in the cores of the Ca II H and K absorption lines. This emission is usually parametrized by the Mount Wilson HK Project's R'_{HK} index [see Baliunas et al. (1998) and references therein]. This index has been shown to be a useful indicator of the levels of jitter in F–M type stars (Saar et al. 1998). Estimates of R'_{HK} are therefore essential to planet search programmes, since they indicate the level of velocity variability in a given star which could be erroneously ascribed to the presence of an unseen planet, rather than jitter.

Unfortunately, while extensive R'_{HK} data are available in the Northern Hemisphere from the Mount Wilson HK Project

programme (Baliunas et al. 1998) and the Vienna-KPNO Ca II H&K Survey (Strassmeier et al. 2000), the only large R'_{HK} data set available in the South is that of Henry et al. (1996). Henry et al. measured chromospheric Ca II emission in more than 800 southern stars (mostly G dwarfs). However, a large fraction of the stars targeted by the Anglo-Australian Planet Search (Tinney et al. 2001; Butler et al. 2001) were not observed by Henry et al. We have therefore begun a programme of ultraviolet (UV) spectroscopy of these stars on the AAT to fill this gap.

2 OBSERVATIONS

The Anglo-Australian Planet Search (AAPS) is being carried out on the 3.9-m Anglo-Australian Telescope (AAT), using the University College London Echelle Spectrograph (UCLES). The observations reported here were obtained on 2001 August 4. For these observations UCLES was operated in its 31 line mm^{-1} mode, with its UV-optimized collimator, to provide an echellogram centred at 390 nm. The detector used was the AAO's EEV 2048 \times 4096 $13.5\text{-}\mu\text{m}$ pixel detector (rather than the MITLL2 2048 \times 4096 $15\text{-}\mu\text{m}$ pixel CCD used for all previous AAPS observations). This CCD provides excellent UV response, with a quantum efficiency at the Ca II HK lines of ≈ 65 per cent. Compared to the MITLL2 the EEV has smaller pixels and reduced charge diffusion, resulting in greatly improved resolution – it will become the default detector for all future AAPS observing. CCD gain was $2.7 \text{ e}^- \text{adu}^{-1}$, and read noise was $4.4 \text{ e}^- \text{pixel}^{-1}$. The CCD was binned by two spatially, to provide an effective slit length of 11 pixel. In the configuration adopted the dispersion at the Ca II R'_{HK} lines is $0.002 \text{ nm pixel}^{-1}$, while the resolution is 3.5 pixel or 0.007 nm.

*E-mail: cgt@aaopep.aao.gov.au

67 F, G, K and M-type stars were observed in 0.7-arcsec seeing through a 1.0×3.5 arcsec² slit, with exposure times ranging from 30 to 180 s, providing a signal-to-noise ratio per 0.002-nm wavelength pixel of between 10 and 50. The stars observed

included AAPS target stars which were also observed by Henry et al. (1996), and stars from the Mount Wilson HK Project, which Henry et al. used as standards for calibrating their observations onto the Mount Wilson R'_{HK} system. The stars observed are listed in

Table 1. AAPS Ca II R'_{HK} targets.

	Star	V	$B - V$	Sp. Typ.	S_{AAT}^a	S_{Henry}^b	S_{MW}^b	$\log R'_{\text{HK,AAT}}$	$\log R'_{\text{HK,CTIO}}^c$	$\log R'_{\text{HK,MW}}^c$	
Calibrators	HD 1835	6.39	0.66	G3V	0.319 ± 0.001	0.343	0.347	-4.49	-4.44	-4.44	
	HD 3795	6.14	0.72	G3/G5V	0.153 ± 0.001	0.146	0.156	-5.06	-5.11	-5.04	
	HD 7570	4.97	0.57	F8V	0.161 ± 0.001	0.161	-	-4.91	-4.95	-	
	HD 10180	7.33	0.63	G1V	0.161 ± 0.002	0.153	-	-4.98	-5.04	-	
	HD 10700	3.49	0.73	G8V	0.163 ± 0.000	0.172	0.171	-5.00	-4.96	-4.96	
	HD 11131	6.72	0.65	G0	0.311 ± 0.001	0.310	0.336	-4.50	-4.47	-4.43	
	HD 13445	6.12	0.81	K0V	0.297 ± 0.001	0.251	-	-4.65	-4.74	-	
	HD 16673	5.79	0.52	F6V	0.209 ± 0.001	0.225	0.215	-4.69	-4.62	-4.66	
	HD 17051	5.40	0.56	G0V	0.240 ± 0.001	0.225	-	-4.61	-4.65	-	
	HD 18907	5.88	0.79	G8/K0V	0.157 ± 0.001	0.109	-	-5.05	-5.40	-	
	HD 20201	7.27	0.58	G0V	0.174 ± 0.001	0.164	-	-4.88	-4.93	-	
	HD 20766	5.53	0.64	G2V	0.262 ± 0.001	0.245	-	-4.60	-4.65	-	
	HD 20782	7.36	0.63	G3V	0.180 ± 0.001	0.176	-	-4.88	-4.91	-	
	HD 20807	5.24	0.60	G1V	0.176 ± 0.001	0.195	-	-4.88	-4.76	-	
	HD 23079	7.12	0.58	F8/G0V	0.155 ± 0.001	0.164	-	-4.99	-4.94	-	
	HD 23249	3.52	0.92	K0IV	0.141 ± 0.000	0.129	0.137	-5.17	-5.22	-5.18	
	HD 25874	6.74	0.67	G5IV-V	0.164 ± 0.001	0.173	-	-4.96	-4.93	-	
	HD 38283	6.69	0.58	G0/G1V	0.153 ± 0.001	0.158	-	-5.01	-4.97	-	
	HD 38973	6.63	0.59	G2V	0.158 ± 0.002	0.175	-	-5.01	-4.88	-	
	HD 202628	6.75	0.64	G5V	0.250 ± 0.001	0.217	-	-4.63	-4.73	-	
	HD 205536	7.07	0.76	G8V	0.162 ± 0.001	0.179	-	-5.01	-4.94	-	
	HD 212168	6.12	0.60	G3IV	0.157 ± 0.001	0.173	-	-4.99	-4.89	-	
	HD 222335	7.18	0.80	K1V	0.233 ± 0.003	0.256	-	-4.78	-4.73	-	
	New Data	HD 142	5.70	0.52	G1IV	0.155 ± 0.001	-	-	-4.95	-	-
		HD 2039	9.00	0.66	G4V	0.176 ± 0.005	-	-	-4.91	-	-
		HD 2587	8.46	0.75	G6V	0.151 ± 0.003	-	-	-5.08	-	-
HD 3823		5.89	0.56	G1V	0.155 ± 0.001	-	-	-4.98	-	-	
HD 6735		7.01	0.57	F8V	0.166 ± 0.002	-	-	-4.91	-	-	
HD 7199		8.06	0.85	K0IV/V	0.180 ± 0.004	-	-	-4.98	-	-	
HD 9280		8.03	0.76	G5	0.150 ± 0.003	-	-	-5.08	-	-	
HD 10647		5.52	0.55	F8V	0.204 ± 0.001	-	-	-4.72	-	-	
HD 11112		7.13	0.64	G4V	0.156 ± 0.001	-	-	-5.02	-	-	
HD 16417		5.78	0.65	G1V	0.147 ± 0.001	-	-	-5.09	-	-	
HD 19632		7.29	0.68	G3/G5V	0.362 ± 0.002	-	-	-4.42	-	-	
HD 20029		7.05	0.56	F7V	0.149 ± 0.001	-	-	-5.02	-	-	
HD 22104		8.32	0.68	G3V	0.154 ± 0.004	-	-	-5.04	-	-	
HD 23127		8.58	0.69	G2V	0.163 ± 0.004	-	-	-4.99	-	-	
HD 23484		6.99	0.87	K1V	0.510 ± 0.002	-	-	-4.43	-	-	
HD 24112		7.24	0.56	F8V	0.152 ± 0.001	-	-	-5.00	-	-	
HD 25587		7.40	0.54	F7V	0.158 ± 0.002	-	-	-4.95	-	-	
HD 26754		7.16	0.55	F7/F8V	0.152 ± 0.001	-	-	-5.00	-	-	
HD 27442		4.44	1.08	K2IV	0.150 ± 0.001	-	-	-5.27	-	-	
HD 28255		6.28	0.66	G4V	0.181 ± 0.001	-	-	-4.89	-	-	
GJ9155B ^d		7.50	0.71	G6V	0.258 ± 0.001	-	-	-4.65	-	-	
HD 30177		8.41	0.77	G8V	0.151 ± 0.004	-	-	-5.08	-	-	
HD 30876		7.49	0.90	K2V	0.469 ± 0.002	-	-	-4.51	-	-	
HD 31527		7.49	0.61	G2V	0.165 ± 0.001	-	-	-4.95	-	-	
HD 36108		6.78	0.59	G3V	0.153 ± 0.002	-	-	-5.01	-	-	
HD 38382		6.34	0.58	F8/G0V	0.162 ± 0.001	-	-	-4.94	-	-	
HD 40307		7.17	0.94	K3V	0.267 ± 0.004	-	-	-4.83	-	-	
HD 204385		7.14	0.56	G0IV	0.158 ± 0.001	-	-	-4.98	-	-	
HD 204961		8.66	1.52	M1V	0.975 ± 0.008	-	-	-5.10	-	-	
HD 205390		7.14	0.88	K2V	0.424 ± 0.002	-	-	-4.53	-	-	
HD 209268		6.88	0.56	F7V	0.153 ± 0.001	-	-	-4.99	-	-	
HD 211317		7.26	0.65	G4IV	0.156 ± 0.002	-	-	-5.03	-	-	
HD 216437		6.04	0.66	G4IV-V	0.154 ± 0.001	-	-	-5.04	-	-	
HD 217987	7.34	1.48	M2/M3V	1.074 ± 0.004	-	-	-5.01	-	-		
HD 222237	7.09	0.99	K3V	0.281 ± 0.007	-	-	-4.86	-	-		

Notes: $a - S_{\text{AAT}}$ calculated as described in Section 3, after calibration onto the Mount Wilson S_{MW} index. $b - S_{\text{Henry}}$ is the Ca II HK index of Henry et al. (1996) (calibrated onto the same scale as the Mount Wilson S_{MW} index), as provided in columns 8–11 of their table 3, and column 14 of their table 4. S_{MW} is the Mount Wilson index used to perform this calibration from columns 4–7 of their table 3. $c - \log R'_{\text{HK,CTIO}}$ are the $\log R'_{\text{HK}}$ indices measured by Henry et al. (1996), while $\log R'_{\text{HK,MW}}$ are the $\log R'_{\text{HK}}$ indices Henry et al. used to check their calibration. $d -$ Also known as SAO258997. This star lies within 6 arcsec of HD 28255 (itself also known as GJ9155A).

Table 1 along with magnitude, colour and spectral type data for each star from the *Hipparcos* catalogue (ESA 1997).

3 ANALYSIS

3.1 Image processing

Reduction of the CCD echellogram images proceeded in a standard manner in the FIGARO environment. Images were overscan subtracted, trimmed and then flat-fielded using flat-field exposures from which the spectrograph blaze function for each order had been fitted and divided out. Scattered light in the spectrograph produces a faint overall level of illumination of the detector – this was fitted in the gaps between orders and subtracted over the whole detector. These images were then straightened to make the echelle orders align with columns on the detector. The entire 3.5-arcsec slit length was then extracted from each order – no sky subtraction was performed. In the wavelength range of interest the sky is featureless. An observation of blank sky obtained well after astronomical twilight reveals sky counts contribute less than $0.016 e^- s^{-1}$ per 0.002-nm wavelength pixel, which is negligible compared to our targets ($\approx 8 e^- s^{-1}$ per 0.002-nm wavelength pixel at $V = 7.5$).

The orders containing the Ca II H and K lines, as well as the adjoining orders (orders 146–142), were then extracted for individual processing. All were wavelength calibrated using a ThAr spectrum obtained at the end of the night. All these data were also flux calibrated using an observation of the *Hubble Space Telescope* flux standard μ Col (Turnshek et al. 1990) – note that we use this observation only to correct the blaze and inter-order sensitivity of our data. The night was not spectrophotometric.

The spectra in order 142 ($\lambda = 398.0$ – 402.6 nm) were cross-correlated against the observation of HD 142, and the barycentric

correction for HD 142 was applied. The result is a set of zero-velocity spectra. [Though HD 142 is a radial velocity variable at the $30 m s^{-1}$ level (Tinney et al. 2002), this variability is negligible for our purposes.] Lastly, all the spectra were re-sampled to the same 0.002-nm binning.

3.2 S indices

The resulting spectra were then used to produce a chromospheric Ca II HK emission index, S_{MW} . The Mount Wilson HK Project defines its S_{MW} (Duncan et al. 1991) as the ratio of the flux in two triangular bands with full width at half-maximum of 0.109 nm centred at 393.3664 (K) and 396.8470 nm (H), to that in two 2.0 nm wide continuum bands centred at 390.1 (V) and 400.1 nm (R). This ratio is measured using a specifically-designed multi-channel photometer. S_{MW} is defined as

$$S_{MW} = \alpha \frac{N_H + N_K}{N_R + N_V},$$

where the N_i are the counts in each of the H, K, V and R bands, and α is a constant determined for each night by the observation of standards.

Using the high-resolution spectra obtained at the AAT, we were able to define our Ca II H and K and continuum bands as having the same effective profiles (i.e. 0.1-nm triangular and 2.0-nm square bandpasses) as used at Mount Wilson (shown in Fig. 1). At the AAT, therefore, we measure the flux in each band, and normalise for the band width, $B(\lambda)$, to obtain

$$N = \frac{\sum_{\lambda} F(\lambda) B(\lambda) \Delta \lambda}{\sum_{\lambda} B(\lambda) \Delta \lambda}$$

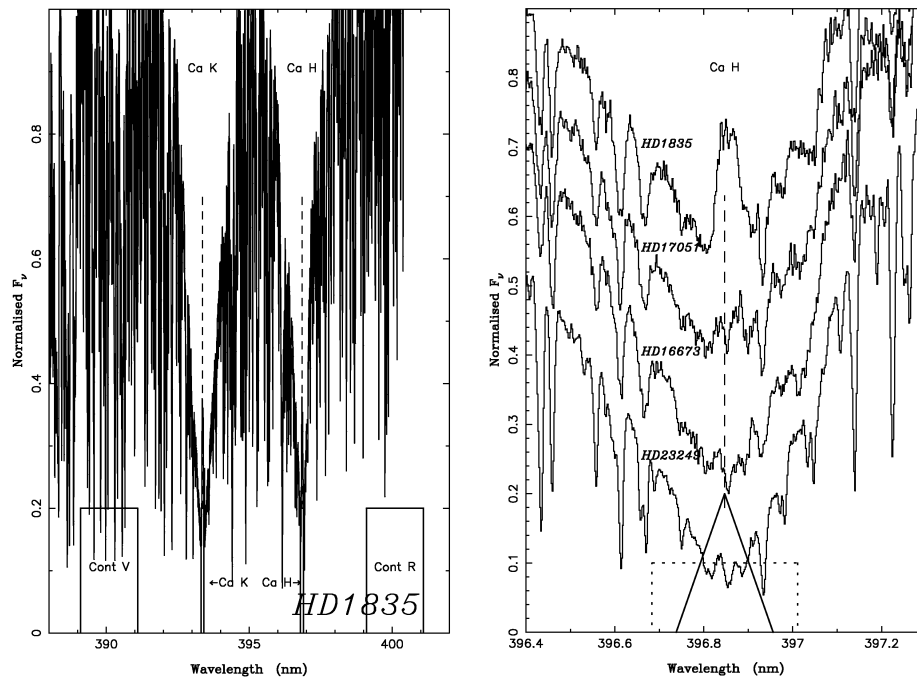


Figure 1. Example Ca II HK spectra from UCLES. The left panel shows an observation of HD 1835, indicating the locations of the Ca II H&K lines, and the continuum V and R regions, described in Section 3.2. The fluctuations seen in this spectrum are due to weak absorption lines, not noise. The right panel shows an expanded region of the Ca II H line for an activity sequence from HD 1835, HD 16673, HD 17051 to HD 23429 (from top to bottom – see Table 1). Also shown are the Mount Wilson triangular Ca II bandpass we have used (solid line), and the Henry et al. (1996) broad Ca II bandpass (dotted line). All spectra have been normalized to $F_v = 1.0$ in the R continuum region. The spectra have been offset by 0.4, 0.1, 0.2, 0.0 (from top to bottom) for clarity.

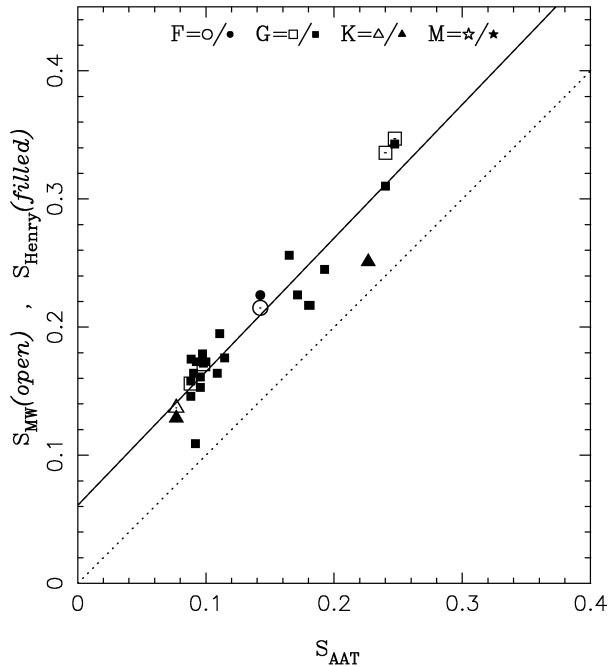


Figure 2. Calibration of the S_{AAT} spectral index on to the S index scale of Mount Wilson (*open symbols*) and Henry et al. (1996) (*filled symbols*) surveys, for the observed calibration objects. Different spectral types are plotted with different symbols. The dotted line shows a unitary transformation, and the solid line is the fitted linear calibration ($S_{\text{MW}} = 1.043S_{\text{AAT}} + 0.061$).

in each band. Because both the Ca H and Ca K lines appear in two orders in our echellogram, we actually obtain two flux estimates for each, which we combine to form an observed S_{AAT} index as follows

$$S_{\text{AAT}} = \frac{N_{\text{H},1} + N_{\text{H},2} + N_{\text{K},1} + N_{\text{K},2}}{2(N_{\text{R}} + N_{\text{V}})}$$

In Fig. 2 we plot this observed S_{AAT} against the S_{MW} and S_{Henry} values reported by Henry et al. A tight linear correlation is seen between S_{MW} and S_{AAT} , with rms scatter about a linear fit of 0.02, zero-point offset of 0.061 and slope of 1.043. Examination of Fig. 2 would suggest that a calibration against the MW data alone would have even smaller scatter, and could be preferred. Certainly our high-resolution spectra should transfer onto the MW system in a linear fashion with no systematic effects. Unfortunately, the number of MW stars accessible in the south is small, so such a calibration would (at present) be based on a small number of stars, and only a few active ones. Because such active stars are by their very nature highly variable in their activity, we have therefore chosen to use *all* the MW and Henry et al. calibrators to derive the relation shown in Fig. 2. No major correlation is seen between degree of deviation from the fit and spectral type.

The values of S_{AAT} so calibrated (including propagated photon-counting uncertainties), and the calibrating S indices are shown in Table 1. In general the scatter about the calibration curve is significantly larger than the photon-counting uncertainties, which likely reflects the intrinsically variable nature of stellar activity.

It should be noted that an advantage of performing these observations at high spectral resolution is that we can define our bandpasses in exactly the same way as those used at Mount Wilson – the resulting indices require only a linear calibration with slope of 1.0 to place them on a standard system. Henry et al., in contrast,

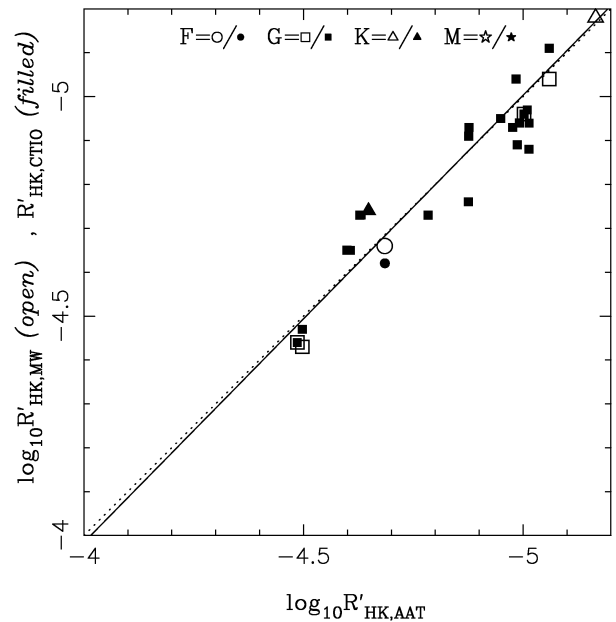


Figure 3. Plot of the derived $R'_{\text{HK,AAT}}$ versus the Mount Wilson (*open symbols*) and Henry et al. (1996) (*filled symbols*) R'_{HK} measurements for our calibration objects. The dotted line shows a unitary transformation, and the solid line is a linear fit.

were forced to use a non-linear calibration, which changes from run to run, introducing possible systematic effects. Experiments on our data show that when the Ca II bandpass is broadened, non-linear calibrations of increasing complexity become necessary, with the consequent risk of introducing systematic uncertainties.

3.3 R'_{HK} indices

The S index provides an estimator of photospheric *plus* chromospheric Ca II strength. For activity purposes, however, it is the chromospheric emission which is of interest. This is usually normalized to the bolometric luminosity of the star, and parametrized by the R'_{HK} index. The derivation of R'_{HK} from S is described in detail in the appendix of Noyes et al. (1984). We follow these procedures to derive the $\log R'_{\text{HK,AAT}}$ values shown in Table 1, where we also show: the $\log R'_{\text{HK,CTIO}}$ values measured by Henry et al. (1996); the $\log R'_{\text{HK,MW}}$ values used to calibrate those data; and the *Hipparcos* $B - V$ photometry used to estimate the photometric contribution to S_{AAT} .

In Fig. 3 we plot $\log R'_{\text{HK,AAT}}$ against $\log R'_{\text{HK,MW}}$ and $\log R'_{\text{HK,CTIO}}$. Note that there are no arbitrary calibration factors included in the transformation from S_{AAT} to $R'_{\text{HK,AAT}}$. The resulting plot is consistent with a unitary transformation – the solid line fit shown in Fig. 3 is for a zero-offset of 0.09 ± 2.3 and a slope 1.02 ± 0.09 , and has rms scatter of 0.09 (for all data), or 0.05 for the MW data alone. We therefore apply no further calibration to our $\log R'_{\text{HK,AAT}}$ estimates, presented in Table 1, but note an rms scatter about the MW standards of ± 0.05 (in the logarithm), which is a better uncertainty estimate for the final results than the photon-counting uncertainties. The rms scatter about the fit for observations in common with Henry et al. is larger at ± 0.09 . Expressed as the ‘mean absolute deviation’ (used by Henry et al.) this corresponds to ± 0.07 , while the mean absolute deviation for the calibration of the Henry et al. sample onto the MW data is ± 0.052 , leading us to conclude a large part of this scatter may be

intrinsic to the Henry et al. comparison sample rather than the AAT data.

4 DISCUSSION

Table 1 provides at least two new R'_{HK} measurements for stars with known planetary companions, HD 27442 (Butler et al. 2001) and HD 142 (Tinney et al. 2002) – though there may be several more, as yet undiscovered, planets in this set of stars (for which AAPS observing is on-going). In the case of HD 27442, we find the star, at this epoch, to be very inactive. Saar et al. (1998) and Santos et al. (2000) have examined the levels of velocity variability intrinsic to stars themselves (σ'_v), as a function of activity (R'_{HK}), in stars monitored by the Lick 3-m planet search. A trend emerges in which more active stars show more intrinsic velocity instability, or ‘jitter’, with a form of $\sigma'_v \propto (R'_{\text{HK}})^{1.1}$ for G and K dwarfs, and with σ'_v in the range $3\text{--}10\text{ m s}^{-1}$ for $\log R'_{\text{HK}} = -5.0$.

Based on this we would predict the jitter in HD 27442 to be $\leq 1.5\text{--}5\text{ m s}^{-1}$. Butler et al. (2001) derive a scatter about their Keplerian fit to the velocity data for HD 27442 of 2.9 m s^{-1} , which is an upper limit to the level of jitter which could be present in this star – in line with its extremely low level of Ca II activity.

HD 142 is only slightly more active at $\log R'_{\text{HK}} = -4.95$, implying an expected level of jitter in the range $\leq 4\text{--}12\text{ m s}^{-1}$. Tinney et al. (2002) report a scatter about a single Keplerian fit of 5.9 m s^{-1} , consistent with this prediction.

Several of the stars in Table 1 reveal themselves to be quite active, with $\log R'_{\text{HK}} > -4.5$. This would correspond to likely levels of jitter greater than $10\text{--}30\text{ m s}^{-1}$ in HD 19632, HD 30876 and HD 205390. Planet candidates detected around stars like this must be scrutinised with great care to avoid erroneous detection claims. The recent results of Queloz et al. (2001) for HD 166435, in particular, provide a valuable cautionary tale. HD 166435 was selected for observation as part of the Observatoire de Haute-Provence ELODIE planet search. The available data (which did not include R'_{HK} measurements) did not indicate particular youth or activity. Over the period 1997 May to 1999 September 70 spectra of this star were acquired, as it appeared to have an unseen planetary companion. Further analysis, however, revealed this variability to be entirely due to activity. A result which is not unexpected when the value of the S index of this star (as measured at Mount Wilson) is considered. At $S = 0.42\text{--}0.51$ (Queloz et al. 2001) this G0 dwarf is phenomenally active – more active than the most active stars shown in Figs 2 and 3, implying $\log R'_{\text{HK}} \approx -4$. At this level of activity the Saar et al. (1998) results would imply an expected level of jitter in the range $36\text{--}120\text{ m s}^{-1}$, which would go much of the way toward explaining the 200 m s^{-1} amplitude velocity variations seen in HD 164435. Having R'_{HK} measurements in hand when considering the validity of a planet candidate is clearly essential.

Finally we would note the intrinsically variable nature of active stars, and the importance of obtaining Ca II observations at multiple epochs in order to be sure a star really *is* inactive. The reliability of such data is important when trying to decide what level of velocity variability could be due to activity/rotation induced jitter, and what level can be trusted to be due to an unseen companion.

5 CONCLUSION

Ca II HK activity measurements are provided for 59 stars from the

Anglo-Australian Planet Search target list – 35 of which are for stars not previously published. 4-m telescope UV echelle spectroscopy is an efficient way in which to obtain high-quality data for this purpose, and because of the high resolution of such data, calibration onto the standard Mount Wilson R'_{HK} system can be carried out with greatly reduced systematic uncertainties.

ACKNOWLEDGMENTS

This paper is based on observations obtained at the Anglo-Australian Telescope, Siding Spring, Australia. The Anglo-Australian Planet Search team would like to gratefully acknowledge the grant of Director’s time in which these observations were carried out, the superb technical support which has been received throughout the programme from AAT staff – in particular E. Penny, R. Patterson, D. Stafford, F. Freeman, S. Lee, J. Pogson and G. Schafer. We further acknowledge support by; the partners of the Anglo-Australian Telescope Agreement (CGT, HRAJ, AJP); NASA grant NAG5-8299 & NSF grant AST95-20443 (GWM); NSF grant AST-9988087 (RPB); and Sun Microsystems.

REFERENCES

- Baliunas S. L., Donahue R. A., Soon W. H., Henry G. W., 1998, in Donahue R. A., Bookbinder J. A., eds, ASP. Conf. Ser. Vol. 154, Cool Stars, Stellar Systems and the Sun. Astron. Soc. Pac., San Francisco, p. 153
- Baranne A. et al., 1996, A&AS, 119, 1
- Butler R. P., Tinney C. G., Marcy G. W., Jones H. R. A., Penny A. J., Apps K., 2001, ApJ, 555, 410
- Duncan D. K. et al., 1991, ApJS, 76, 383
- ESA, 1997, *The Hipparcos and Tycho Catalogues*, ESA SP-1200
- Fischer D. A., Marcy G. W., Butler R. P., Vogt S. S., Frink S., Apps K., 2001, ApJ, 551, 1107
- Henry T. J., Soderblom D. R., Donahue R. A., Baliunas S. L., 1996, AJ, 111, 439
- Kürster M., Endl M., Els S., Hatzes A. P., Cochran W. D., Döbereiner S., Dennerl K., 2000, A&A, 353, L33
- Naef D., Mayor M., Pepe F., Queloz D., Santos N. C., Udry S., Burnet M., 2001, A&A, 375, 205
- Noyes R. W., Hartmann L. W., Baliunas S. L., Duncan D. K., Vaughan A. H., 1984, ApJ, 279, 763
- Queloz D., Mayor M., Sivan J. P., Kohler D., Perrier C., Marotti J. M., Beuzit J. L., 1998, ASP Conf. Ser. Vol. 134, Brown Dwarfs and Extrasolar Planets. Astron. Soc. Pac., San Francisco, p. 324
- Queloz D., Rebolo R., Martin E. L., Zapatero Osorio M. R., 2001, A&A, 379, 279
- Saar S. H., Fischer D., 2000, ApJ, 534, L105
- Saar S. H., Butler R. P., Marcy G. W., 1998, ApJ, 498, L153
- Santos N. C., Mayor M., Naef D., Pepe F., Queloz D., Udry S., Blecha A., 2000, A&A, 361, 265
- Strassmeier K. G., Washuettl A., Granzer Th., Scheck M., Weber M., 2000, A&AS, 142, 275
- Tinney C. G., Butler R. P., Marcy G. W., Jones H. R. A., Penny A. J., Vogt S. S., Apps K., Henry G. W., 2001, ApJ, 551, 507
- Tinney C. G., Butler R. P., Marcy G. W., Jones H. R. A., Penny McCarthy C., Carter B. D., 2002, ApJ, in press (astro-ph/0111255)
- Turnshek D. A., Bohlin R. C., Williamson R. L., Lupie O. L., Koorneef J., 1990, AJ, 99, 1243
- Vogt S. S., Marcy G. W., Butler R. P., Apps K., 2000, ApJ, 536, 902

This paper has been typeset from a $\text{\TeX}/\text{\LaTeX}$ file prepared by the author.